Proton Binding and Dipole Moment of Hemoglobin. Refined Calculations*,†

William H. Orttung

ABSTRACT: Theoretical calculations of the titration curve and dipole moment of hemoglobin by the extended Tanford–Kirkwood theory have been improved by using Perutz' 1968 atomic coordinates, by including ionic strength effects, and by allowing distributions with multiple as well as single-jump excitations of the protons from the most stable assignment. The best fit of the titration curve was obtained by assuming the sites to be at the protein surface in the calculation of coulomb interactions. In comparison with the earlier calculations, the proton binding of the carboxyl and histidine sites was lower on the alkaline side. The calculated dipole moment also increased smoothly from pH 6 to 8, in agreement with the data. The latter behavior resulted from the pH dependence of the mean moment rather than the fluctuation moment.

The calculated tyrosine titrations were in poor agreement with the spectrophotometric titration data. The sources of this discrepancy were found to be hydrogen bonding and site masking effects that had not been included in the calculations. Comparative results for human and methemoglobin, for the $\alpha_1\beta_1$ half-molecule, and for the α and β quarter-molecules are also discussed.

The investigations described below were originally undertaken to provide an understanding of Kerr effect dispersion data on horse hemoglobin (Orttung, 1965). Properties such as the dielectric constant and Kerr effect are related to the distribution of charge within the protein and to the fluctuations of the protons among the available binding sites at each pH. An understanding of these properties requires, first of all, an understanding of the titration curve. The titration curve of a protein solution measures the total number of hydrogen ions bound to the protein as a function of pH. The many aspects of the interpretation of titration data have been carefully reviewed (Tanford, 1962).

A theoretical method of evaluating the effect of coulomb interactions on proton binding was available (Tanford and Kirkwood, 1957; Tanford, 1957) and was extended to allow the evaluation of the proton binding by the individual sites (Orttung, 1968a–c). According to the Tanford–Kirkwood approach, the sites are represented as point charges in a dielectric sphere immersed in the solvent medium. The binding averages are taken over the possible configurations of charge, weighted according to their coulomb energy. Exploratory calculations were then carried out for the hemoglobin system (Orttung, 1969a–c), demonstrating the feasibility of this approach to the problem and suggesting that useful information concerning the titrations of the individual sites could be obtained. Two recent developments have allowed major improvements in the calculations: First, the atomic coordinates from the 2.8-Å resolution electron density map of horse oxyhemoglobin became available (Perutz *et al.*, 1968), and were substituted for the less certain estimates from the earlier model (Perutz, 1965; Orttung, 1969a). Second, a newer computer, more powerful by almost an order of magnitude, became available and allowed the consideration of nonzero ionic strengths, as well as more than three times as many proton distributions among the available sites. The latter capability allowed multiple as well as single-jump excitations of the protons from the most stable assignment, thus permitting calculations above pH 9 and for species such as methemoglobin in which several pK values lie close together. The additional distributions were also found to be important for nonzero ionic strengths.

The new results support the earlier calculations in a qualitative way, but many of the details are significantly different. A more extensive comparison with the data at higher pH and ionic strength has also become possible, and interesting conclusions have been drawn, particularly with respect to the tryosine titration.

Recently, Perutz *et al.* (1969) have shown that large movements of the side chains occur in the oxy to deoxy transition and are of major importance to the Bohr effect. Needless to say, the effect of such motions cannot be included in detailed calculations of the titration curve until coordinate information becomes available, so that consideration of the Bohr effect in the present paper must be restricted to observations based on the oxyhemoglobin coordinates (Perutz *et al.*, 1968) and the effect of rigid rotation of the subunits to the deoxy form (Muirhead *et al.*, 1967; Bolton *et al.*, 1968).

It might also be pointed out that the present calculations assume the same geometry at all pH values. Whether or not such an assumption is justified, the calculations at least suggest what might be predicted for such a model. Compara-

* From the Department of Chemistry, University of California, Riverside, California 92502. *Received September 24, 1969.* Supported by Public Health Service Research Grant GM 11683 from the Division of General Medical Sciences. Presented in part at the 158th National Meeting of the American Chemical Society, New York, N. Y., Sept 1969, Abstract BIOL-279.

† Material supplementary to this Article has been deposited as Document No. NAPS-00930 with the ASIS National Auxiliary Publication Service, c/o CCM Information Corp., 909 3rd Ave., New York, N. Y. 10022. A copy may be secured by citing the document number and by remitting $2.00 for microfiche or $6.00 for photocopies. Advance payment is required. Make checks or money orders payable to: CCM-IC-NAPS.

tive results for the myoglobin system are presented elsewhere (W. H. Orttung, in preparation, 1970).

Theoretical Methods

The methods used in the calculations have been described (Orttung, 1968a–c). To take advantage of the greater capabilities of a newer computer, the programs were improved in three ways:

(1) The effect of nonzero ionic strengths on the coulomb interactions was included; (2) the number of allowed distributions was increased to include multiple-jump as well as single-jump proton excitations; and (3) the output was improved for the case of molecules with no symmetry. The following paragraphs summarize the first two of these improvements, and the third is for molecules such as myoglobin (W. H. Orttung, in preparation). A more detailed report giving program descriptions and FORTRAN listings is available as a supplement to the original report (Orttung, 1968c).

Nonzero Ionic Strengths. We may start from eq 43, 44, and 63 of Orttung (1968a) in the form

$$\frac{\langle W_{\nu,}{}^{(x)}\rangle}{kT} = \frac{1}{\Omega_\nu{}^{(i)}} \sum_{(x) \text{ of } (i)} \sum_{l=1}^{n_{st}} \left\{ \sum_{m>l}^{n_{st}} \varphi_{lm}{}' - \frac{e^2}{2akT} \xi_l{}^2 C_{ll} \right\} \quad (1)$$

The contribution of C_{lm} to $\varphi_{lm}{}'$ for $l \neq m$ is of the following form.

$$\varphi_{lm}{}' = \xi_l \xi_m \frac{e^2}{bkT} \left[(A_{lm} - B_{lm}) - \frac{b}{a} C_{lm} \right] \quad (2)$$

A suitable expression for C_{lm} was given by Tanford and Kirkwood (1957) in their eq 8. Test calculations of C_{lm} up to $x = 1$ agreed with the results presented in Figure 2 of their paper. It was found that a value of $n = 20$ was necessary for x values up to 4, and the value, $n = 20$, was used in all of the calculations. (n is the summation index in Tanford and Kirkwood's eq 8; κ is the reciprocal ion atmosphere radius; a is the distance of closest approach of counterions to the center of the protein, which is assumed to be a sphere of radius b for this purpose ; and $x = \kappa a$.)

Multiple-Jump Excitations. In the earlier calculations (Orttung, 1968b, 1969a), only single-jump excitations from the most stable distribution were allowed. Sites of each type were assigned a k value, with $k = 1$ corresponding to the most strongly binding type. Placing ν protons on the n_{st} sites in order of increasing k value, sites of type k_ν were then partially occupied. The earlier calculations allowed only excitation jumps of the type $k_\nu - 1$ to k_ν or k_ν to $k_\nu + 1$. The total number of distributions considered for a given ν was then $1 + m_1 + m_2$, where m_1 and m_2 were the maximum number of protons allowed to participate in each type of jump. In addition to the limitations on m_1 and m_2 arising from the available number of sites of each type, an externally supplied limit was also provided for each k value so that calculation times could be controlled.

The calculations have now been generalized to include multiple-jump excitations. Let k_i and k_f be the initial and final k values for a jump. It is then convenient to introduce the two indices i_d and i_f defined as in eq 3 and 4. The number pair, $i_d i_f$, then characterizes a jump relative to k_ν; alternatively,

$$i_d = k_f - k_i \quad (3)$$

$$i_f = k_f - k_\nu \quad (4)$$

the pair $i_d k_i$ is an absolute specification. Although i_d could be as large as $k_{max} - 1$ when $k_i = 1$, only values less than or equal to 4 have been allowed in the calculations. As many as 14 types of jump are then possible, as illustrated in Table I by the array of $i_d i_f$ values, for which k_ν has been taken as 5.

TABLE I: $i_d i_f$ Values.

	k_i								
i_d	1	2	3	4	5	6	7	8	9
1				10	11				
2			20	21	22				
3		30	31	32	33				
4	40	41	42	43	44				

In analogy to the earlier calculations, which considered 10 or 11 excitations separately, the present calculations also consider one type of excitation at a time, so that there are $1 + m_{10} + m_{11} + \ldots + m_{43} + m_{44}$ excitations for each ν. In addition, provision has been made for $(m_{10} + m_{11})/d$ simultaneous single-jump excitations with each multiple-jump excitation, where d was taken as i_d if not explicitly specified in a particular calculation. The externally supplied limits now take the form of a double array of numbers $n_{i_d k_i}$ and $d_{i_d k_i}$. For comparison, only n_{1k_i} had to be specified in the earlier calculations.

Calculations

Site Coordinates. The atomic coordinates of the 2.8-Å resolution model of horse oxyhemoglobin (Perutz *et al.*, 1968) were used directly except for the minor modifications listed below. Perutz' coordinates were permuted so that c^*,a,b, corresponded to x,y,z. The latter convention was used in the earlier work (Orttung, 1969a) and caused the z axis to be the twofold symmetry axis.

Coordinates were chosen for the proton binding sites in the following manner, and hopefully represent the location of the coulomb charge. A point midway between the oxygens was taken for the carboxyl group, and the nitrogen atom was used in the RNH_2 sites. For histidine, tyrosine, and arginine, atoms Nϵ2, Oη, and Cζ were chosen, respectively. The only site whose coordinates were modified from Perutz' listing was the β-chain N-terminal amino, whose $z(b)$ coordinate was increased by 2 Å to increase its separation from His H24(146)β from 2.7 to 4.0 Å. Only eight pairs of sites remained separated by less than 4 Å. These were: Lys H10(127)α–Asp A4(6)α, 2.2 Å; His G19 (117)β–Glu B8(26)β, 2.6 Å; His G19(112)α–Glu B8(27)α, 3.0 Å; Lys E9(65)β–Glu B2(20)β, 3.1 Å; Lys H22(139)α–His FG1(89)α, 3.2 Å; His E13(69)β–Glu E17(73)β, 3.3 Å; Arg C6(40)β–Trp C7(42)α, 3.5 Å; and His CD3(45)α–heme COO PL(4)α, 3.8 Å.

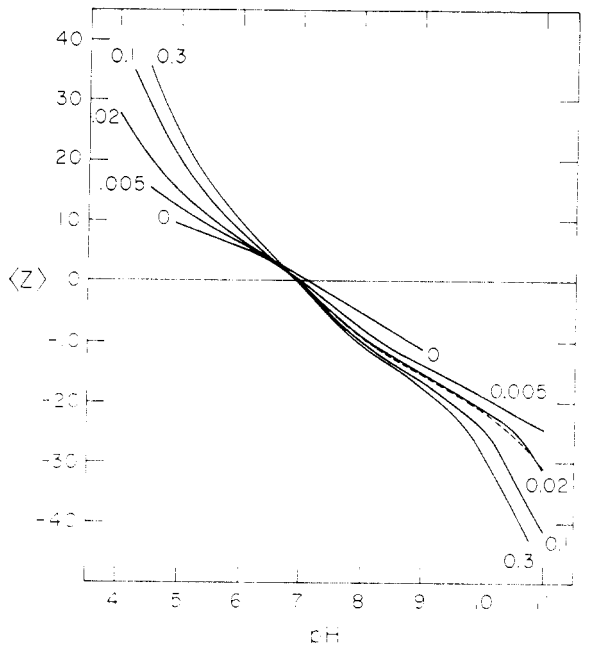

FIGURE 1: Theoretical titration curve of horse oxyhemoglobin tetramer as a function of ionic strength. The effect of allowing simultaneous single excitations with the multiple excitations is shown by the dashed line for 0.02 ionic strength.

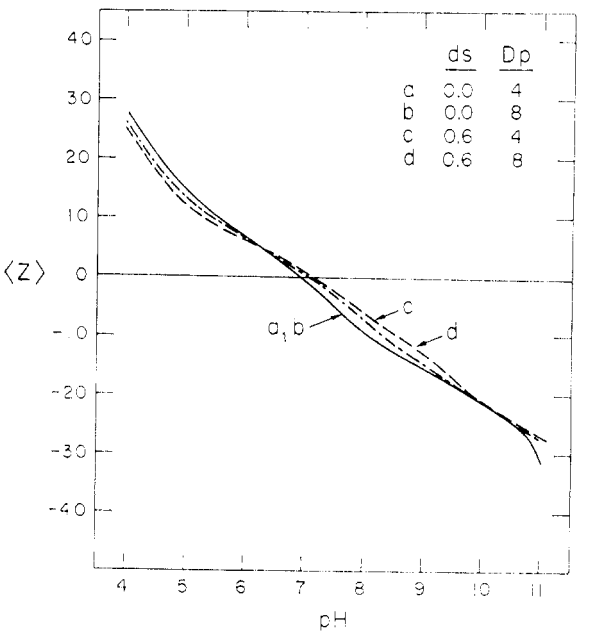

FIGURE 2: Sensitivity of the theoretical titration curve to variation of the assumed site depth, d_s, and protein dielectric constant, D_p, at 0.02 ionic strength.

To obtain site coordinates representing deoxyhemoglobin the subunits were rotated as rigid units as in the earlier calculations (Orttung, 1969a), according to the 5.5-Å resolution data (Muirhead *et al.*, 1967; Bolton *et al.*, 1968). Side-chain motions of the type recently discovered by Perutz *et al.* (1969) were not considered. The centers of mass for the oxy and deoxy structures were calculated to be on the *b* axis at −1.19 and −1.17 Å, respectively.

To obtain site coordinates representing human oxyhemoglobin, Arg Gl8(116)β was converted into His Gl8(116)β without changing the site coordinates; His NA2(2)β and Asp F6(85)α were added and assigned site coordinates (x,y,z = 9.23, 7.60, 22.58, and 16.99, −4.92, −17.04, respectively, in the c^*,a,b system) and His El3(69)β, His E20(76)β, Asp Al3(16)β, Glu B2(20)β, Glu H3(125)β, and Asp F3(82)α were removed. The deoxy coordinates were generated in the same way as for horse hemoglobin.

Intrinsic pK's and Other Parameters. The intrinsic pK's chosen were essentially the same as before (Orttung, 1969a), and are shown in Table II along with a listing of the number of sites of each type (n_{sk}) for the species considered. Tanford (1962) has given a careful discussion of the problem of assigning intrinsic pK's. The possibility that glutamic and aspartic acid side-chain carboxyls might have slightly different

TABLE II: Number of Sites and Assumed Intrinsic pK's for Horse and Human Met- and Oxyhemoglobin.

k			Assumed	n_{sk}	
Met	Oxy	Site Type	pK_{int}	Horse	Human
1	1	Arg	12.50	14	12
2	2	Lys	10.20	44[a]	44
3	3	Tyr	9.60	12	12
4	4	Cys[g]	9.10	2	2
5		FeOH[b]	8.00[b]	4[b]	4[b]
6	5	Nta[c]	7.80	4	4
7	6	His[d]	6.00	30	30
8	7	Coo[e]	4.80	68	62
9	8	Ctc[f]	3.75	4	4

[a] Including E9α. [b] Methemoglobin only. [c] N-Terminal amino. [d] Excluding E7 and F8. [e] Includes Asp, Glu, and heme propionic carboxyls. [f] C-Terminal carboxyl. [g] Excluding G11α.

TABLE III: Illustrative Sets of Externally Supplied Excitation Limits (If Unspecified, $d_{i_d k_i} = i_d$).

	$n_{i_d k_i}$; Subscript: $d_{i_d k_i}$							
	k_i							
i_d	1	2	3	4	5	6	7	8
	Horse Oxyhemoglobin							
1	2	6	2	2	4	10	0	
2	0	2	4_1	2_1	4_1	0		
3	0	2	4_1	2_1	0			
	Horse Methemoglobin							
1	2	6	2	2	4	4	10	0
2	0	2	4_1	2_1	4_1	4_1	0	
3	0	2	4_1	2_1	2_2	0		
4	0	2	4_1	0	0			

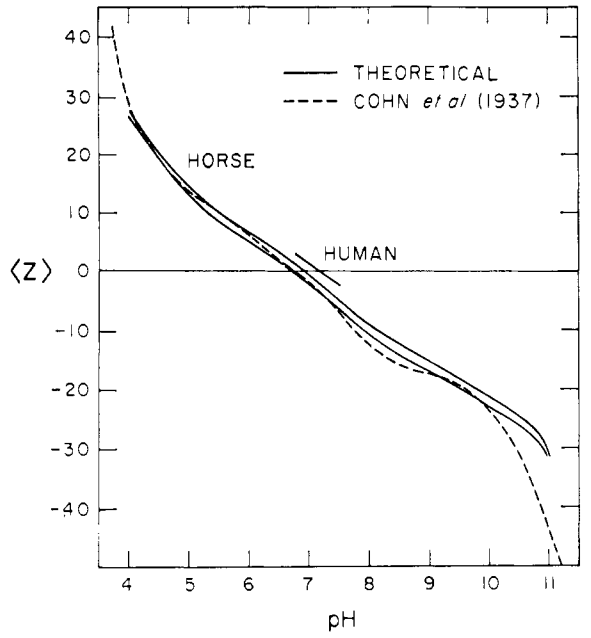

FIGURE 3: Comparison of theoretical and experimental results for horse oxy- (or carboxy-) hemoglobin at low ionic strength and 25°. The theoretical curves are for 0.02 ionic strength, the lower curve being for the species without Lys E9(60)α in either chain. The data of Cohn *et al.* (1937) have been shifted upward by 3.0 charge units to give the correct isoionic pH. The data correspond to no added salt. The theoretical result for human oxyhemoglobin at 0.02 ionic strength is also shown near the isoionic pH for comparison with the data of Tanford and Nozaki (1966).

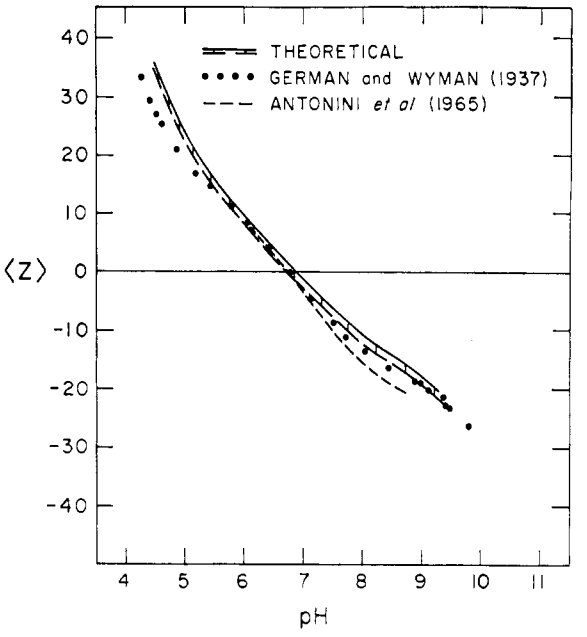

FIGURE 4: Comparison of theoretical and experimental results for horse oxyhemoglobin near an ionic strength of 0.3 at 25°. The effect of excluding Lys E9(60)α is also estimated. The experimental data of German and Wyman (1937) is at 0.333 M NaCl, and the data of Antonini *et al.* (1965) is at 0.25 M NaCl.

intrinsic pK's (Nozaki and Tanford, 1967) has not been recognized in our calculations because of computer time and storage limitations. A temperature of 25°, solvent dielectric constant of 78.4, and protein radius of 28 Å were used for all of the calculations. To evaluate the coulomb interactions, the assumed depth of sites within the protein was varied, but the best results were obtained with the sites on the surface. A protein dielectric constant of 4 was used. The results were insensitive to this parameter with the sites on the surface. The distance of closest approach of counterions was taken as 29.5 Å, *i.e.*, as b + 1.5 Å. Radii used for the half- and quarter-molecules were b = 22.2 and 17.5 Å, respectively. The results were essentially independent of small variations of the assumed b values.

Calculation Planning. All calculations were done with the individual site average approximation (Orttung, 1968a, 1969a). The IBM 360/50 computer usually required about 8 hr to calculate results based on 1200–1700 distributions for a molecule like hemoglobin (about 180 sites with twofold rotation symmetry). It was therefore of importance to know how many distributions would occur for each ν value so that suitable lower and upper limits, ν_l and ν_h, could be chosen for a given set of externally supplied excitation limits. This information was obtained by a skeleton program that calculated only the number of distributions for each ν. Table III shows sample sets of externally supplied distribution limits. None of the runs used more distributions than allowed by the samples in Table III, and some runs used considerably fewer.

Results

Ionic Strength and Parameter Dependence. Calculations for horse oxyhemoglobin at a range of ionic strengths are shown in Figure 1. The molecule was assumed to maintain the same tetrameric structure at all ionic strengths and pH's. The distributions were limited essentially as shown in Table III, but without simultaneous single distributions. Inclusion of the latter had a small smoothing effect at high pH. For the conditions of the calculations, the ion atmosphere radius, $1/\kappa$, was given in terms of the ionic strength, μ, by $3.04/\mu^{1/2}$, and ranged from 43 Å at μ = 0.005 to 5.5 Å at μ = 0.3.

Figure 2 illustrates the sensitivity of the results to parameter variation. As will be seen below, case a of Figure 2 (sites at the surface, protein dielectric constant of 4) gave the best agreement with the titration and dielectric data while case c was the least satisfactory. Small variations of the intrinsic pK's were also made. These variations had more straightforward effects than in the earlier calculations (Orttung, 1969a), and the values of Table II seemed to give the best fit.

Comparison with Titration Data. Figures 3–6 show comparisons between the theoretical values and experimental data from various sources. In Figures 3–5, the theoretical values are slightly high at pH 8–9 and perhaps a little low at pH 5–7. The alkaline discrepancy is also found for the isolated subunits in Figure 6, suggesting that it may not be related to subunit interactions. The tyrosine masking effect shown in Figure 5 is discussed in the following section.

The comparison of theoretical curves for tetramer and dimer in Figure 7 suggests a possible explanation for the low values on the acid side, since it is known that the tetramer dissociates into dimers as the pH is lowered from 6.5 to 4.5 (Rossi-Fanelli *et al.*, 1964). The greater proton binding of

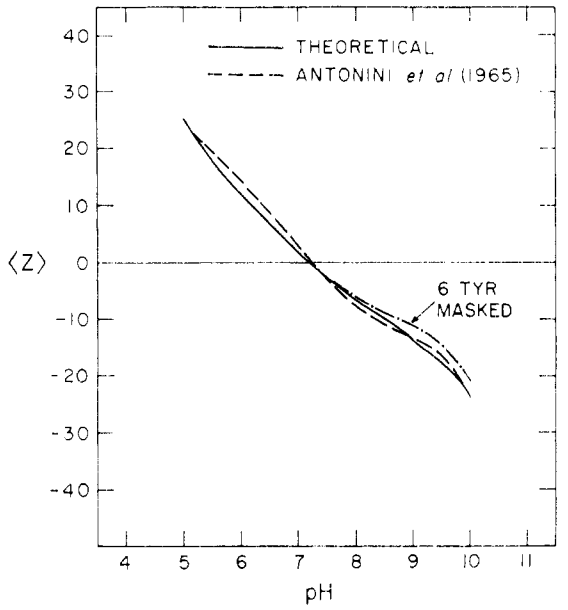

FIGURE 5: Comparison of theoretical and experimental results for human oxyhemoglobin at 0.25 M NaCl at 25°. The data of Antonini *et al.* (1965) were shifted upward by 1.47 charge units, as suggested by Tanford and Nozaki (1966). The six tyrosines masked in the second calculation were the H23α, H23β, and C7α pairs.

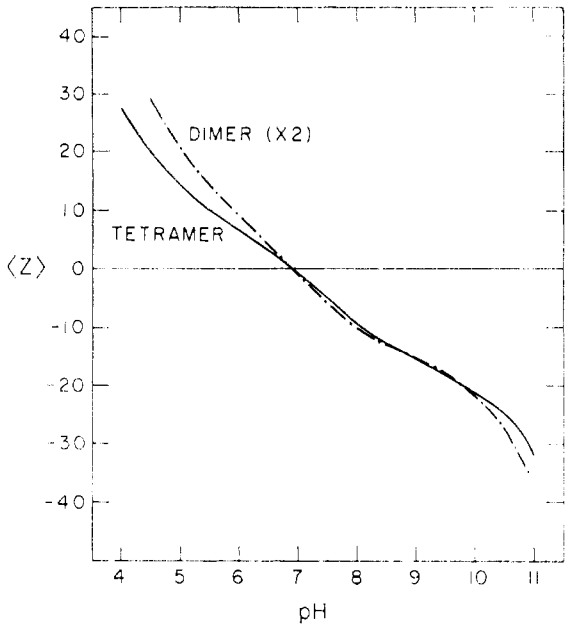

FIGURE 7: Comparison of the theoretical titration curve of the $\alpha_1\beta_1$ dimer with that of the tetramer for horse oxyhemoglobin at 0.02 ionic strength.

the dimer at low pH is to be expected as a general consequence of the acid-driven dissociation (Wyman, 1964). The decreased proton binding of the dimer above pH 10 is also consistent with the observed alkaline dissociation. It is interesting that the dimer and tetramer have the same titration curve in the region of tetramer stability.

In Figure 3, the theoretical isoionic pH for human hemoglobin is found to be 7.2, compared with a value of 6.8 for horse hemoglobin. The difference of 0.4 pH units is in excellent agreement with the data of Tanford and Nozaki (1966). The predicted ionic strength dependence of the isoionic point for horse hemoglobin (Figure 1) is negative, as compared to the slightly positive shift with increasing NaCl concentration found by Scatchard and Pigliacampi (1962).

Decomposition of the Theoretical Titration Curves. Figures 8–10 show the theoretical contributions to the titration

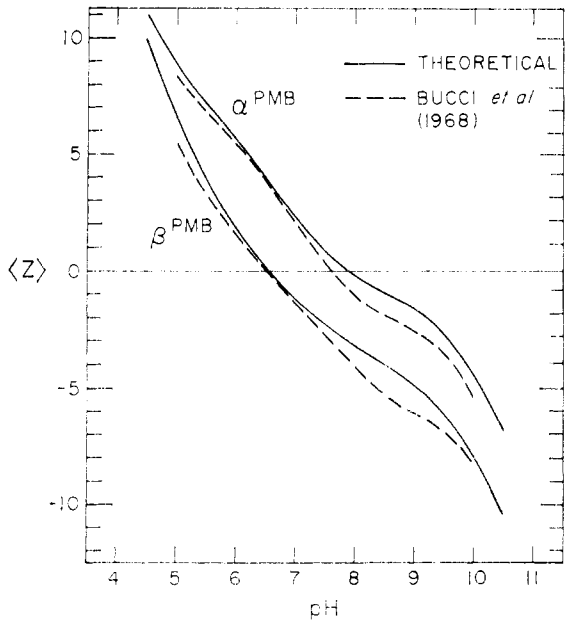

FIGURE 6: Comparison of theoretical and experimental results for human α and β subunits in the CO form with cysteine residues masked by *p*-mercuribenzoate at 0.25 ionic strength (Bucci *et al.*, 1968). The data was taken at 20°, and the calculation was for 25°.

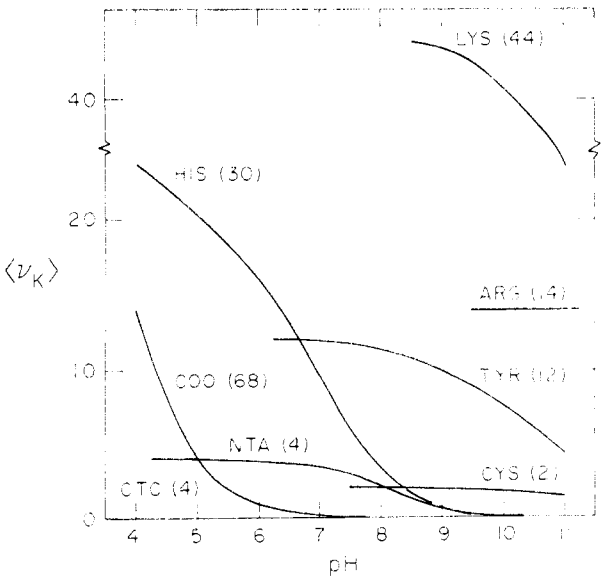

FIGURE 8: Theoretical number of protons bound by each type of site for horse oxyhemoglobin at 0.02 ionic strength. The number of sites of each type is shown in parentheses.

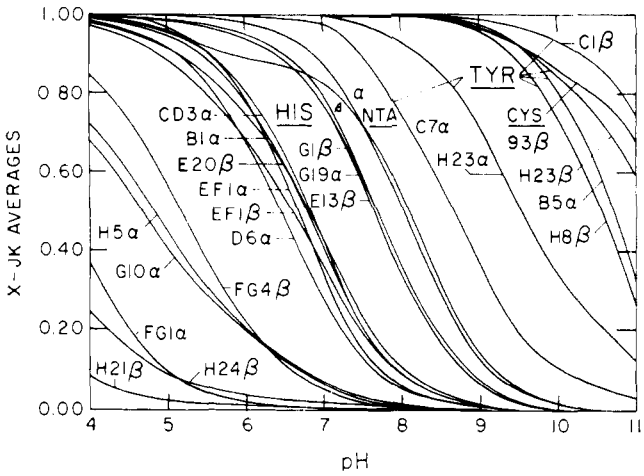

FIGURE 9: Theoretical titration curves of the histidine, N-terminal amino, cysteine, and tyrosine sites for horse oxyhemoglobin at 25° and 0.02 ionic strength for the species containing two Lys E9(60)α sites.

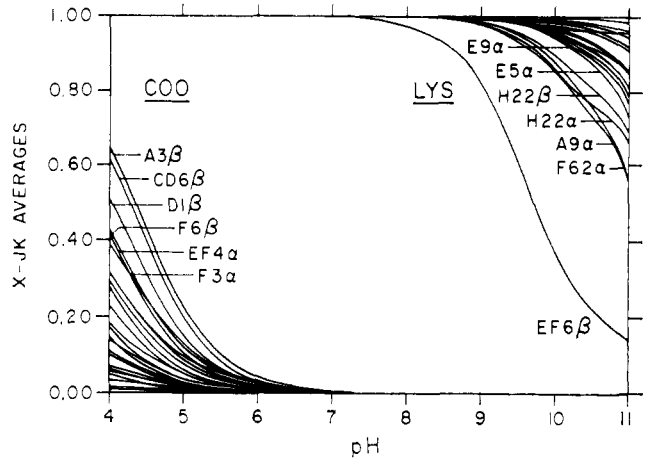

FIGURE 10: Theoretical titration curves of the carboxyl and lysine sites for the system described in Figure 9.

curve for the case of horse oxyhemoglobin at 0.02 ionic strength. In comparison with the earlier calculations (Orttung, 1969a), the alkaline ends of the carboxyl and histidine titrations are much lower. The individual histidine sites again vary widely, but there are no longer any very strongly binding carboxyls. The reduction of the carboxyl binding relative to the older calculations is apparently due to a subtle redistribution of the site separations in the 5- to 15-Å range. In the new coordinates, the positive and negative sites are much more uniformly arranged than in the earlier model. The change in histidine binding is mainly due to the change of assumed site depth (from 0.6 to 0 Å) in the evaluation of coulomb interactions. Lys EF6(82)β has a very low apparent pK because it is only 4.7 Å from its twofold rotated twin. Cys F9(93)β has a high apparent pK because it is 5–6 Å away from Asp FG1(94)β and the β-chain C-terminal carboxyl, and also because it is near Tyr H23(145)β. The latter site is undoubtedly masked, as suggested in the following paragraph.

The experimental tyrosine spectrophotometric titration data is compared with two theoretical predictions in Figure 11. The discrepancy of four to six charge units between the first prediction and the data is partly explained by the inclusion of all twelve sites in the calculation. The data strongly suggest that four sites (one per subunit, probably the H23 residues) are buried and do not titrate. A similar experimental result in the case of myoglobin (Hermans, 1962) has been verified by a crystallographic study of iodinated met myoglobin (Kretsinger, 1968), in which it was shown that Tyr 23H was buried. An additional contribution to the discrepancy may arise from the two Tyr C7(42)α residues, which are very close (~3 Å) to the positively charged Arg C6(40)β sites according to Perutz' coordinates. In our calculations, which consider only coulomb interactions between the sites, the proton does not bind to Tyr C7α above pH 8. However, M. F. Perutz (1969, personal communication) has pointed out that Tyr C7α forms a hydrogen bond with the carbonyl oxygen of Asn G4(97)α in both the oxy and deoxy structures. Apparently the hydrogen bond is sufficiently strong to override the coulomb repulsion effect predicted by our calculations.

In the second calculation shown in Figure 11, six sites (H23α, H23β, and C7α) were masked (removed from the calculation), and the resulting theoretical curve is in much better agreement with the data. The improvement in the total titration curve is shown in Figure 5. In addition, the apparent pK of Cys F9(93)β was shifted downward from 9.75 to 9.50, in closer agreement with an expected value near 9 (Adler and Cecil, 1966). A similar change was obtained when the low ionic strength calculation shown in Figure 8 was repeated: Masking the six tyrosines lowered the apparent pK of cysteine to about 10.5.

From Figure 9, it may be seen that both N-terminal

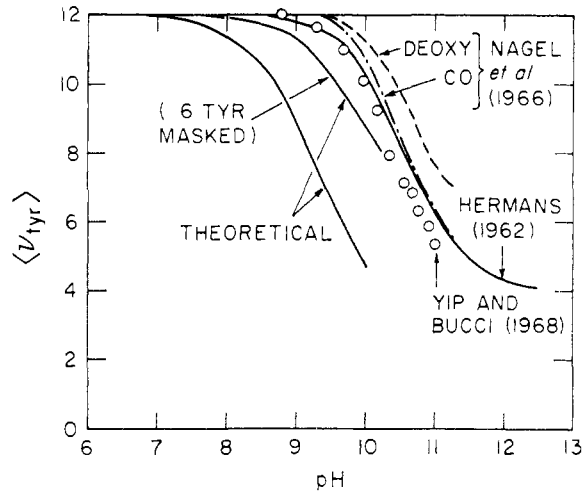

FIGURE 11: Comparison of the theoretical tyrosine titration of human oxyhemoglobin at 25° and 0.25 ionic strength with the available spectrophotometric data. The data of Hermans (1962) refer to horse or human CO hemoglobin in a phosphate–carbonate buffer of about 0.7 ionic strength. Nagel *et al.* (1966) used human CO and deoxyhemoglobin at 0.1 ionic strength. Yip and Bucci (1968) studied human CO hemoglobin at 20° and 0.25 ionic strength. The six tyrosines masked in the second calculation were the H23α, H23β, and C7α pairs.

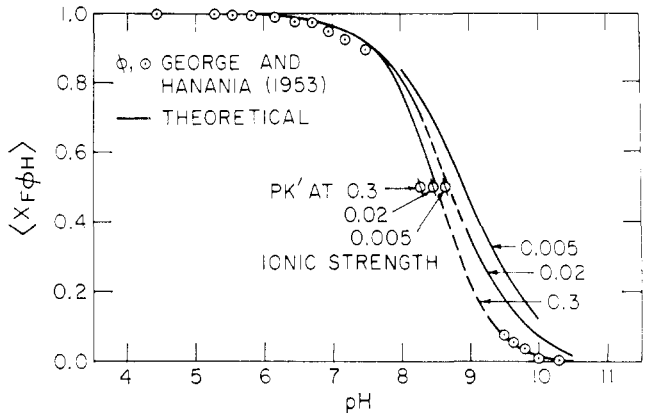

FIGURE 12: Comparison of the theoretical titrations of the FeOH sites of horse methemoglobin at 25° and various ionic strengths with the data of George and Hanania (1953). The data points (O) were at 20°, and 0.26 ionic strength. The theoretical calculations assumed an intrinsic pK of 8.0 for the FeOH sites. The theoretical binding of the β-chain sites was 10–15% greater than that of the α-chain sites.

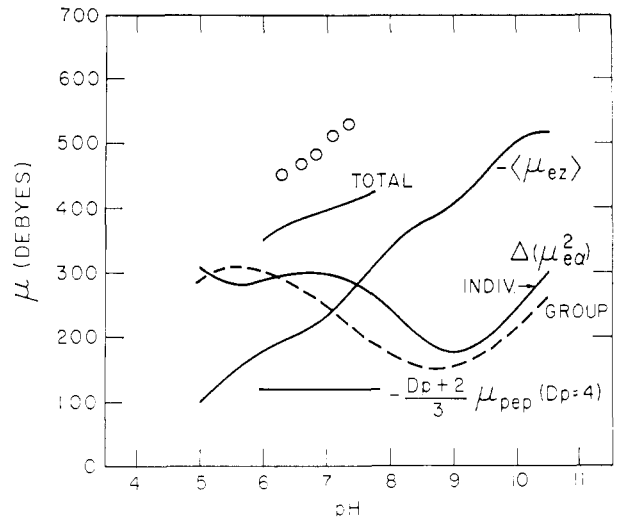

FIGURE 13: Comparison of the theoretical root-mean-square dipole of horse methemoglobin at 25° and 0.02 ionic strength with the data (O) of Goebel and Vogel (1964) at 20° and low ionic strength. The various contributions to the theoretical result are shown in the figure. The discrepancy between the data and the total moment from the sources shown would be removed by an additional contribution to either the fluctuation or mean moment.

amino groups have apparent pK's slightly above 8, in contrast to the earlier results, in which the α-N-terminal amino had an apparent pK of 7. The new results are therefore not in good agreement with the apparent pK of 6.7 for the α-N-terminal amino obtained by Hill and Davis (1967) from the pH-dependent reaction with fluorodinitrobenzene. Perutz' coordinates for the N-terminal amino groups are still uncertain, so that the explanation for this difference between calculation and data must be sought later.

Methemoglobin. Calculations for methemoglobin were carried out using the same site coordinates as for the oxy form, except that FeOH sites were positioned at the iron atoms and assigned an intrinsic pK of 8.0 (Tanford, 1962). The calculated change of the titration curve from horse oxy- to methemoglobin differed from the experimental data of Wyman and Ingalls (1941) by less than half a pH unit shift to the alkaline side.

The calculated average titration of the FeOH sites is compared with spectrophotometric titration data in Figure 12 for three ionic strengths. Again, the calculated values are shifted to the alkaline side by about 0.25 pH unit, but the pH dependence of the apparent pK and the shape of the curve at 0.3 ionic strength are in good agreement with the data. It is clear that agreement with the data would have been obtained if the intrinsic pK had been assigned a value of 7.7 rather than 8.0. George and Hanania (1953) also observed very small inflections in the FeOH spectral titration corresponding to apparent pK's of 5.1 and 6.3. Our calculations were not complete in this region, but examination of Figures 9 and 10 shows that there are two groups of histidines titrating with approximately these pK's. It is possible that one or more of these histidines is responsible for the pK's observed in the FeOH titration.

Beetlestone and Irvine (1964a) determined the apparent pK's of human hemoglobin A, S, and C by a spectrophotometric method and found that $\Delta pK(A\text{–}C) \leqq 2\,\Delta pK(A\text{–}S) \leqq 0.06$ at 0.02 ionic strength. These three hemoglobins differ only in residue A3(6)β, having Glu, Val, and Lys, respectively. This site is approximately 36 or 54 Å from the α-chain irons, and 34 or 37 Å from the β-chain irons. It was then shown in an approximate calculation that the Tanford–Kirkwood theory of electrostatic interactions was capable of explaining the observed ΔpK's (Beetlestone and Irvine, 1964b). We have repeated the calculation using the new coordinates and an ionic strength of 0.02, and have found $\Delta pK(A\text{–}C) = 0.03$ (0.02 for the α-chain sites, and 0.04 for the β-chain sites). The new calculations automatically include the "charge buffering effect" (Beetlestone and Irvine, 1968) and predict slightly smaller differences than observed.

Dipole Moment. The theoretically predicted contributions to the root mean-square dipole moment of horse methemoglobin at low ionic strength are compared with the available data in Figure 13. $\langle \mu_{ez} \rangle$ is the mean dipole moment along the twofold axis arising from the proton binding sites; $\Delta(\mu_{e\alpha}^2)$ is the contribution to the mean-square dipole moment arising from proton fluctuations among the available sites; D_p is the dielectric constant of the protein; and μ_{pep} is the contribution of the peptide group bond dipoles to the mean dipole moment. (The contribution of bond dipoles from side chains was not considered.) The difference in $\Delta(\mu_{e\alpha}^2)$ as calculated by the individual site average or by the group average approximation is an indication of the effect of correlation of charge fluctuations at the different binding sites. (The first approximation does not include correlation effects; the second recognizes them in an approximate way.) The method of evaluating the various contributions mentioned above has been described earlier (Orttung, 1969b). The theoretical value has the correct pH dependence, in contrast to the earlier results (Orttung, 1969b), but is about 100 D smaller than the data.

The theoretical results attribute the pH dependence to the mean moment rather than to the fluctuation moment. The correct pH dependence was not obtained until the

sites were placed at the surface in the evaluation of the coulomb interactions. (The same change also improved the fit of the titration curve. See Figures 2–5.) The earlier calculations (Orttung, 1969a,b) had assumed the sites to be 0.6 Å below the surface for this purpose. The mean moment contribution may also account for part of the difference between the pH dependence in the case of ovalbumin and bovine serum albumin and predictions of the fluctuation moment based on the Kirkwood–Shumaker theory (Takashima, 1965).

The discrepancy of about 100 D in the root-mean-square moment could arise in part from a side-chain contribution to both the mean and fluctuation moments. No attempt has been made to include this effect in the theoretical estimates. There may also be a contribution from ion atmosphere polarization effects, although Krause and O'Konski (1963) found no definite evidence for such an effect in the observed relaxation times of small proteins.

Bohr Effect. With no *ad hoc* assumptions about site masking in either the oxy or the deoxy structure, an alkaline Bohr effect was predicted upon rigid rotation of the subunits to the deoxy form. The source of this effect was the separation of the Arg C6β and Tyr C7α sites by the subunit rotation. However, M. F. Perutz (1969, personal communication) has pointed out that Tyr C7α is hydrogen bonded to the Asn G4α carbonyl in both the oxy and deoxy forms, so that the calculated effect is apparently not found in the real system.

A negative Bohr effect at pH 7–9 involving the β-chain N-terminal amino group was also predicted upon rigid rotation of subunits to the deoxy structure. The source of this effect (in our calculations) was the C-terminal carboxyl of the other β chain, which increased its distance from the N-terminal amino from 6 to 13 A in the oxy–deoxy structural change. It is not clear at this time whether this effect is actually a contributor to the observed Bohr effect. The large heat of ionization of the amino group, 11–14 kcal/mole (Tanford, 1962), may or may not be compatible with the observed 7–9 kcal for the alkaline Bohr effect and approximately 0 kcal for the acid Bohr effect (Antonini *et al.*, 1965).

The contributions of side-chain motions to the Bohr effect, recently discovered by Perutz *et al.* (1969), have not been included in the calculations. It may be suggested, however, that the dimer–tetramer equilibrium is responsible for part of the observed acid Bohr effect. This possibility arises because (1) the dimer binds protons more strongly than the tetramer (Figure 7); (2) the dissociation of oxyhemoglobin is about 50% between pH 5 and 6 (Rossi-Fanelli *et al.*, 1964), the same pH range in which the acid Bohr effect is observed; and (3) deoxyhemoglobin is considerably less dissociated to dimer than the oxy form (Guidotti, 1967). Figure 7 predicts that the difference of proton binding between dimer and tetramer keeps increasing as the pH is lowered. However, the proton binding of the deoxy tetramer is predicted to be higher than that of the oxy tetramer below pH 5, according to our calculations, so that the combination of the above effects could lead to a maximum of the acid Bohr effect between pH 5 and 6. Further speculation concerning the various possible contributions to the Bohr effect should undoubtedly await the detailed X-ray studies of both the oxy and deoxy forms.

Discussion

The most striking change from the earlier calculations (Orttung, 1969a) was the reduction of the carboxyl and histidine binding on the alkaline side. The carboxyl reduction was traced to relatively subtle changes in the site coordinates which had the effect of distributing the positive and negative charges more evenly. The histidine reduction was partly explained by the change of assumed site depth from 0.6 Å in the earlier calculations to 0.0 Å in the present calculation of the coulomb interactions. Not only was the fit of the titration data improved by placing the sites on the surface, but the correct pH dependence of the root-mean-square dipole moment was also obtained. The latter effect was caused by the mean moment, rather than by the fluctuation moment.

Since the site depth and protein dielectric constant parameters provide an oversimplified description of the real protein–solvent interface, the greatest remaining internal deficiency of the calculations seems to be the model used for evaluating the coulomb interactions. The possibilities of hydrogen bonding and/or site masking (or burying) provide a further source of potential disagreement between the data and calculations. Problems of this type seem to be most severe in the case of tyrosine sites.

On a more general level, the use of atomic coordinates from the crystalline state in calculations for a dilute solution may be questioned. There does not seem to be any evidence that the structure of hemoglobin or myoglobin undergoes a large change from crystal to solution, although small shifts of side chains may well occur either upon dilution or upon change of the pH. The calculations presented here are then best regarded as a reference to which the data may be compared.

References

Adler, A., and Cecil, R. (1966), *Biochem. J. 101*, 741.

Antonini, E., Wyman, J., Brunori, M., Fronticelli, C., Bucci, E., and Rossi-Fanelli, A. (1965), *J. Biol. Chem. 240*, 1096.

Beetlestone, J. G., and Irvine, D. H. (1964a), *Proc. Roy. Soc., Ser. A 277*, 401.

Beetlestone, J. G., and Irvine, D. H. (1964b), *Proc. Roy. Soc. Ser. A 277*, 414.

Beetlestone, J. G., and Irvine, D. H. (1968), *J. Chem. Soc. A*, 951.

Bolton, W., Cox, J. M., and Perutz, M. F. (1968), *J. Mol. Biol. 33*, 283.

Bucci, E., Fronticelli, C., and Ragatz, B. (1968), *J. Biol. Chem. 243*, 241.

Cohn, E. J., Green, A. A., and Blanchard, M. H. (1937), *J. Amer. Chem. Soc. 59*, 509.

George, P., and Hanania, G. (1953), *Biochem. J. 55*, 236.

German, B., and Wyman, J. (1937), *J. Biol. Chem. 117*, 533.

Goebel, W., and Vogel, H. (1964), *Z. Naturforsch. B 19*, 292.

Guidotti, G. (1967), *J. Biol. Chem. 242*, 3685.

Hermans, Jr., J. (1962), *Biochemistry 1*, 193.

Hill, R. J., and Davis, R. W. (1967), *J. Biol. Chem. 242*, 2005.

Krause, S., and O'Konski, C. T. (1963), *Biopolymers 1*, 503.

Kretsinger, R. H. (1968), *J. Mol. Biol. 31*, 315.

Muirhead, H., Cox, J. M., Mazzarella, L., and Perutz, M. F. (1967), *J. Mol. Biol. 28*, 117.

Nagel, R. L., Ranney, H. M., and Kucinskis, L. L. (1966), *Biochemistry 5*, 1934.
Nozaki, K., and Tanford, C. (1967), *J. Biol. Chem. 242*, 4731.
Orttung, W. H. (1965), *J. Amer. Chem. Soc. 87*, 924.
Orttung, W. H. (1968a), *J. Phys. Chem. 72*, 4058.
Orttung, W. H. (1968b), *J. Phys. Chem. 72*, 4066.
Orttung, W. H. (1968c), Document No. 10070, ADI Auxiliary Publications Project, Photoduplication Service, Library of Congress, Washington, D. C. See Orttung (1968b), for ordering information.
Orttung, W. H. (1969a), *J. Amer. Chem. Soc. 91*, 162.
Orttung, W. H. (1969b), *J. Phys. Chem. 73*, 418.
Orttung, W. H. (1969c), *J. Phys. Chem. 73*, 2908
Perutz, M. F. (1965), *J. Mol. Biol. 13*, 646.
Perutz, M. F., Muirhead, H., Cox, J. M., and Goaman, L. C. G. (1968), *Nature 219 (London)*, 131.
Perutz, M. F., Muirhead, H., Mazzarella, L., Crowther, R. A., Greer, J., and Kilmartin, J. V. (1969), *Nature (London) 222*, 1240.
Rossi-Fanelli, A., Antonini, E., and Caputo, A. (1964), *Advan. Protein Chem. 19*, 73.
Scatchard, G., and Pigliacampi, J. (1962), *J. Amer. Chem. Soc. 84*, 127.
Takashima, S. (1965), *J. Phys. Chem. 69*, 2281.
Tanford, C. (1957), *J. Amer. Chem. Soc. 79*, 5340.
Tanford, C. (1962), *Advan. Protein Chem. 17*, 69.
Tanford, C., and Kirkwood, J. G. (1957), *J. Amer. Chem. Soc. 79*, 5333.
Tanford, C., and Nozaki, Y. (1966), *J. Biol. Chem. 241*, 2832.
Wyman, J., Jr. (1964), *Advan. Protein Chem. 19*, 223.
Wyman, J., and Ingalls, E. N. (1941), *J. Biol. Chem. 139*, 877.
Yip, Y. K., and Bucci, E. (1968), *J. Biol. Chem. 243*, 5948.

Actin–Heavy Meromyosin Binding. Determination of Binding Stoichiometry from Adenosine Triphosphatase Kinetic Measurements*

A. A. Rizzino, W. W. Barouch, E. Eisenberg,† and C. Moos

ABSTRACT: Enzyme kinetic measurements of the effects of actin on the heavy meromyosin adenosine triphosphatase (ATPase) are used for a study of the binding of heavy meromyosin to actin. In the absence of free magnesium ions, the potassium-activated ATPase of heavy meromyosin is inhibited by actin, and this inhibition is used as a quantitative measure of binding. The activation of the heavy meromyosin ATPase by actin in the presence of magnesium ions is also used as a measure of binding. Both kinds of data, when analyzed according to the theory of multiple equilibria, give simple binding curves with a binding stoichiometry of 1 mole of heavy meromyosin/mole of monomers in F-actin.

It is generally accepted that the molecular basis for the contraction of muscle is an interaction between the two major contractile proteins, actin and myosin (Szent-Györgyi, 1951; Huxley, 1960, 1969); however, there is still considerable question about one of the most fundamental features of the actin–myosin interaction, namely, the stoichiometric binding ratio of the actin to the myosin. The number of monomers in F-actin which interact with each myosin molecule is of particular interest because myosin probably contains two active subunits (Stracher and Dreizen, 1966; Slayter and Lowey, 1967; Lowey *et al.*, 1969; Nauss *et al.*, 1969) which, when separated from the molecule as subfragment 1, are both capable of binding actin (Mueller and Perry, 1962; Young, 1967). The actin monomers, on the other hand, are single polypeptide chains (Rees and Young, 1967). On this basis, one might expect that each myosin molecule would have two binding sites for actin and would combine with two monomers in the F-actin filament.

Unfortunately, it is difficult to investigate the actin–myosin binding directly under physiological conditions because myosin aggregates at low ionic strength, but experiments can be carried out at high ionic strength where myosin is disaggregated, or using heavy meromyosin, an early proteolytic digestion product of myosin which retains the actin binding and ATPase-active region of the myosin intact but does not aggregate at low ionic strength (Szent-Györgyi, 1953). On the basis of electron microscope observations of the actin–heavy meromyosin complex, Huxley (1963) concluded that each actin monomer could bind one molecule of heavy meromyosin. However, while some studies of actin–

* From the Department of Biochemistry, State University of New York, Stony Brook, New York 11790. *Received February 9, 1970.* Supported by National Institutes of Health Research Grant GM-10249, by National Institutes of Health Predoctoral Fellowships GM-38534 (A. A. R.) and GM-43089 (W. W. B.), by National Science Foundation Undergraduate Research Participant award to A. A. R. for 1967, and by an Advanced Research Fellowship from the American Heart Association, supported by the Heart Association of Suffolk County, N. Y. (E. E.). Preliminary reports of some of this work have been presented (Rizzino *et al.*, 1968; Eisenberg *et al.*, 1969).

† Present address: Laboratory of Biochemistry, Cellular Physiology Section, National Heart Institute, Bethesda, Md. 20014.